INSTITUTE OF PHYSICS PUBLISHING PLASMA SOURCES SCIENCE AND TECHNOLOGY

Plasma Sources Sci. Technol. **16** (2007) 110–115 doi:10.1088/0963-0252/16/1/015

Soft x-ray generation in gases by means of a pulsed electron beam produced in a high-voltage barier discharge

A V Azarov, P J M Peters and K-J Boller

Laser Physics and Nonlinear Optics Group, Faculty of Science and Technology, University of Twente, PO Box 217, 7500 AE, Enschede, The Netherlands

E-mail: A.V.Azarov@tnw.utwente.nl

Received 6 June 2006, in final form 8 October 2006
Published 12 December 2006
Online at stacks.iop.org/PSST/16/110

Abstract

A large area pulsed electron beam is produced by a high-voltage barrier discharge. We compare the properties of the x-rays generated by stopping this beam of electrons in a thin metal foil with those generated by stopping the electrons directly in various gases. The generation of x-rays was investigated in He, Ne and Ar with and without an Al foil in the discharge chamber. It appears that, for voltages of up to 15 kV used in our experiments, x-rays are produced by the 'bremsstrahlung' mechanism and that characteristic x-ray radiation does not play an important role. The x-ray intensity strongly depends on the parameters of the electron beam (electron energy and current density) and the stopping material properties (Z-number). The energy of the x-ray photons is comparable to the applied voltage. The highest obtained energy in the x-ray spectrum depends on the electron energy (∼10 keV in the investigated case) and the lowest energy is determined by the transmittance of the output window and the window of the detector.

1. Introduction

Homogeneous gas discharges working at multi-atmospheric pressures, as used for example in gas laser technology, require a reliable and efficient source for gas preionization. One of the possible solutions is to utilize x-ray radiation as the preionization source. For a good performance of a high-pressure gas laser the x-ray source should produce a wide and homogeneous x-ray beam, which homogeneously preionizes the entire discharge volume. In addition, the x-ray beam should create a sufficiently high initial electron density within the entire discharge volume before the discharge is ignited. Hard x-ray radiation (hundreds keV or higher) shows only a low absorption, particularly in gas, and therefore is rather inefficient for preionization. In comparison, the absorption coefficient is much larger for soft x-rays, which makes a high flux of soft x-ray photons very attractive for preionizing high-pressure gas mixtures.

Usually x-rays are produced by decelerating electrons or beams of electrons in a stopping medium, most of the time a medium with a high mass density.

Recently the possibility of generating a broad electron beam in an open barrier discharge has been reported [1, 2]. The advantages of this type of electron beam generation are that the generated electrons are fast, with an energy approximately equal to the discharge voltage, and that the energy efficiency of the e-beam generation is as high as 90% [3]. Other advantages are that such discharges are very stable, with a high shot-to-shot reproducibility, although the area of the produced beam is rather large (10–100 cm^2). The open barrier discharge is a modification of the so-called 'open' discharge, proposed in the early 1980s by the group of Bokhan and thoroughly investigated until now, e.g. see the recent publications [4, 5]. A typical open discharge unit includes a plane metal cathode and a plane perforated metal anode (usually a mesh), separated by a narrow (∼1 mm) gas gap, and a field-free drift space behind the anode. In the open barrier discharge the cathode is made of a dielectric material. This modification improves the discharge stability at high current density. However, the electron acceleration in the open barrier discharge is achieved by means of the so-called 'runaway' effect, as well as in the

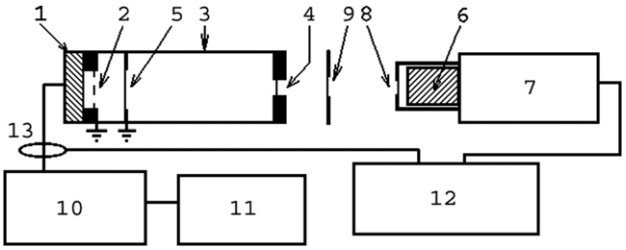

Figure 1. The experimental setup. 1: dielectric cathode, 2: metal anode grid, 3: discharge chamber, 4: Kapton output window, 5: Al target, 6: scintillator, 7: photomultiplier, 8: Al input window, 9: Al attenuator, 10: triggering unit, 11: high-voltage power supply, 12: oscilloscope, 13: current transformer.

usual open discharge. An overview on this runaway effect is presented in [6].

In the present paper, we report on an investigation of x-ray generation by means of this kind of fast electron beams in specific gases and metals. The x-ray generation has been observed by stopping the beam electrons both directly in a gas and in a metal target placed in the e-beam. The dependence of the x-ray intensity on gas pressure and charging voltage has been investigated in helium, neon and argon discharges. It has been found that the observed x-rays is not characteristic radiation but bremsstrahlung radiation.

2. Experimental setup

The main features and electrical properties of the open barrier discharge with a dielectric cathode and a perforated metal anode are described in [1]. Further investigations led to an improved setup described in [2]. Except for small modifications all the experiments presented in this report were made with this setup.

The setup is shown schematically in figure 1. The main part of the electron beam generator is a dielectric cylinder (1) with a diameter of 5.3 cm and a thickness of 2.15 cm made of ceramic with a high dielectric constant ($\varepsilon \sim 4300$). For these parameters, the specific capacitance of the dielectric is $\sim 0.17\,\mathrm{nF\,cm^{-2}}$, while its breakdown voltage is $\sim 30\,\mathrm{kV}$. A metallic electrode is fixed on the rear side of the dielectric. The diameter of the active area of the dielectric cathode is 41 mm. A metal grid (2) of 41 mm diameter is placed 3 mm apart from the cathode and held by a metal ring. The metal ring and the metal grid serve as a composed anode. An Al foil (5) with a thickness of $\sim 13\,\mu$m and a diameter of 38 mm could be fixed inside the discharge chamber by a metal ring 17 mm apart from the grid. This foil then serves as the target to stop fast electrons and to generate x-rays. Both the anode and the foil are grounded in this case. For experiments aiming at generating x-rays directly in the gas, the Al foil is removed. The whole discharge setup is encapsulated in a discharge chamber (3) made of a glass tube 0.5 m long. The output window (4) with a diameter of 1 cm is made of a 0.1 mm thick Kapton foil. Several pieces of Al foil (9), ~ 1 cm in diameter, placed 3 mm behind the output window, serve as variable attenuator for x-rays during the experiments.

The dielectric also serves as the energy storage capacitor and is charged by a Hipotronics R50B high-voltage power supply (11) through a $10\,\mathrm{M\Omega}$ resistor. A TGI1 1000/25 thyratron in the triggering unit (10) is used to trigger the discharge.

A photomultiplier Philips 56AVP (7) attached with a piece of scintillating plastic NE102 (6) is used as an x-ray detector. The scintillator is placed in a special box with an input window (8) of diameter ~ 1 cm made out of 13 μm thick Al foil to prevent illumination of the photomultiplier by ambient light or by light from the discharge.

A Rogovski coil Pearson Electronics Inc. (13) (model 110, 0.1 V/A) is used to measure the current waveforms. The current waveforms as well as the x-ray signals detected by the photomultiplier are captured by a digital oscilloscope Tektronix TDS 640A (12).

The x-ray signal amplitude depended on the photomultiplier amplification coefficient governed by the supply voltage. In order to minimize the experimental error in the x-ray intensity measurements, the amplification of the photomultiplier in every experiment was chosen such that the signal amplitude is much higher than the noise level but well below the saturation level. The effective amplification for the photomultiplier varies for all figures 3–9, but it is the same in each individual figure. Thus the curves in the same figure can be directly compared. The experimental error in the measured amplification coefficient as well as in the x-ray signal amplitude fluctuation is given by the error bars in all the figures.

The generation of x-rays was investigated in He, Ne and Ar with and without an Al foil in the discharge chamber. The discharge chamber was filled with a fresh gas before each new series of experiments on a particular gas or gas pressure. The electron beam device can be operated at a repetition rate of up to several kHz but usually a repetition rate of about 1 Hz was used in our experiments.

3. Experimental results

The plastic scintillator NE102 is originally designed for maximum efficiency and linearity in the MeV-range ($\sim 1.2 \times 10^4$ photons $\mathrm{MeV^{-1}}$). We decided to use this scintillator also in the keV-range, although here the efficiency is much lower and the linearity is not specified. The reason is the fast rise and fall time of the scintillator (specified as 0.9 and 2.6 ns, respectively). The response time of the photomultiplier was measured (with short light pulses from a red emitting LED) to be ~ 5 ns. The measurement of x-ray pulses was performed using the 100 MHz bandwidth setting of the oscilloscope. This results in uni-polar (negative voltage) signal pulses from the photomultiplier as shown in figure 2, with a temporal width of ~ 13 ns (FWHM), for a discharge in Ar at a pressure of 4 mbar without Al foil in the discharge chamber. The shape and the half-width of the x-ray pulse waveform are almost independent of the charging voltage, type of gas used and the way the x-rays are generated, either in a gas or in an Al target. However, the signal amplitude and the delay of the x-ray signal with regard to the discharge current and voltage depend on the above mentioned parameters.

First the x-ray signal, produced in a discharge in He without an Al foil in the chamber, was measured as a function of the discharge voltage at three different gas pressures. The measured dependence of the detected x-ray signal on the discharge voltage is shown in figure 3, where the gas pressure

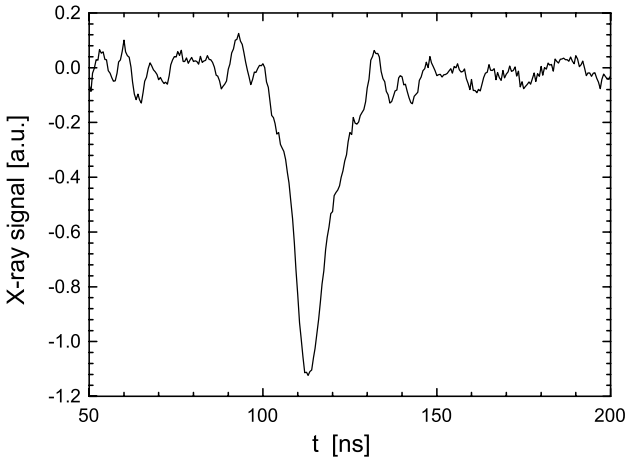

Figure 2. Typical waveform of the x-ray signal detected by the photomultiplier. Discharge in Ar at pressure 4 mbar. Charging voltage is 15 kV. The x-rays are produced in Ar without an Al foil inside the discharge chamber.

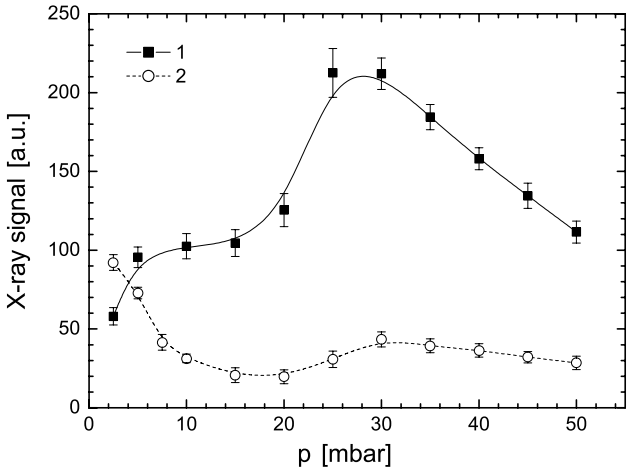

Figure 4. Dependence of the x-ray signal amplitude on He pressure. The charging voltage is 15 kV. 1: with Al foil inside the discharge chamber, 2: without Al foil.

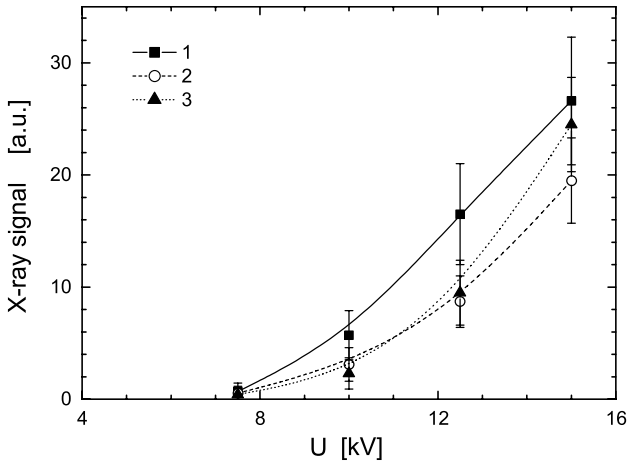

Figure 3. Dependence of the x-ray signal, generated in the discharge in He without an Al foil placed inside the discharge chamber, on the discharge voltage. The gas pressure is 25 (1), 20 (2) and 15 mbar (3).

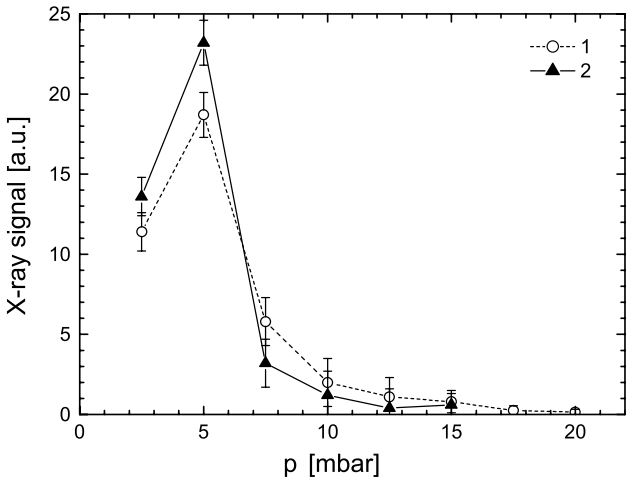

Figure 5. Dependence of the x-ray signal amplitude on Ne pressure. Charging voltage is 15 kV. 1: with Al foil inside the discharge chamber, 2: without Al foil.

is 25 (1), 20 (2) and 15 mbar (3). It is seen that for our configuration the x-ray generation has a threshold value at around 8 kV and increases at higher voltages.

Then we measured the x-ray signals with and without the Al foil inside the discharge chamber for different gases and at different pressures. The dependence of the x-ray signal on the He pressure, with a constant discharge voltage of 15 kV, is shown in figure 4. In case (1) the electrons were stopped by the Al foil placed in the discharge chamber, while in case (2) the x-ray radiation was produced by the deceleration of electrons in He gas (here the Al foil was removed from the discharge chamber). At a pressure higher than 10 mbar both the curves show the same behaviour such as a maximum at about 30 mbar but the x-ray signal without the foil is about 5 times smaller. On the other hand, at pressures below 10 mbar the x-ray signal without the foil rises and even surpasses the signal obtained with foil (at a few mbar). We believe that this is due to x-rays generated by the stopping of electrons in the walls of the chamber. When the gas pressure decreases the mean free path and thus the penetration depth of the fast electrons in the gas increases, as is seen from the visible glow of the gas excited by fast electrons. At low gas pressure the visible glow of the gas occupies a larger volume up to almost the entire volume of the chamber. Hence more fast electrons are scattered towards the wall of the chamber causing x-ray generation.

For the discharges in Ne the same experiments led to different results as shown in figure 5. In case (1) the electrons were stopped by the Al foil placed in the discharge chamber (see figure 1) and in case (2) the x-ray radiation was produced by the deceleration of electrons in Ne. The charging voltage was 15 kV. In both cases the signal amplitudes are almost equal, over the entire observed pressure range. The maximum x-ray signal was observed at a gas pressure of ∼5 mbar in both cases.

For comparing the x-ray generation in the Al foil with different types of gases, we recorded the pressure dependence for He (trace 1), Ne (2) and Ar (3) (see figure 6). We note that the maximum x-ray signal is almost the same in all the gases; however, the gas pressure of the maximum x-ray signal decreases with increasing atomic weight of the gas.

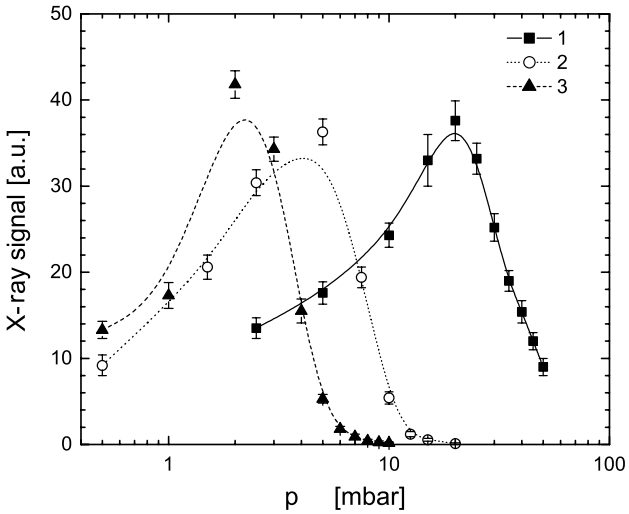

Figure 6. Dependence of the x-ray signal amplitude generated in Al foil target on gas pressure. Charging voltage is 15 kV. 1: He, 2: Ne, 3: Ar.

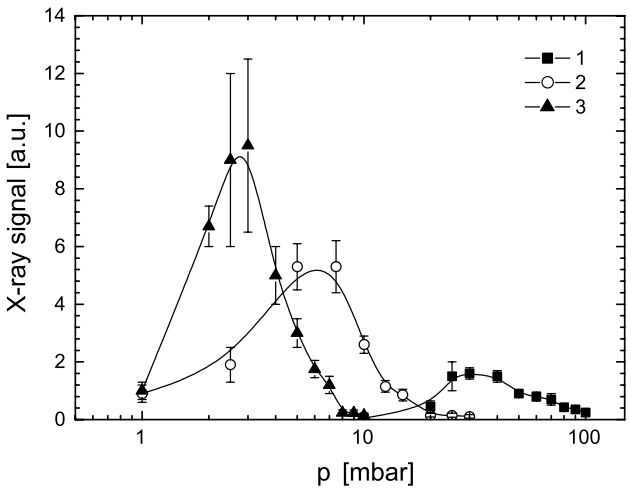

Figure 7. Dependence of the x-ray signal amplitude generated in gases without an Al foil target on gas pressure. Charging voltage is 15 kV. 1: He, 2: Ne, 3: Ar.

Specifically, in He the maximum x-ray signal is observed at a pressure of ∼25 mbar, in Ne at ∼5 mbar and in Ar at ∼2.5 mbar. We believe that this observation of equal maximum signal is due to, on the one hand, the same charging voltage and, on the other hand, the use of the same stopping material for the generated electrons, namely the Al foil, for all the three experiments.

Next we compared the x-ray generation directly in the gas (the Al foil was removed) for the same three gases (see figure 7). The three curves shown in the figure correspond to He (trace 1), Ne (2) and Ar (3). Again it can be seen that the gas pressure at which the maximum x-ray signal is observed decreases with increasing atomic weight of the gas. Again, in He the maximum x-ray signal is observed at ∼25 mbar, in Ne at ∼5 mbar and in Ar at ∼2.5 mbar. However, the maximum x-ray generation is observed in Ar while He shows the least efficient conversion of e-beam energy into x-ray radiation. In figure 7 there is no increase in the x-ray signal in He (1) plotted at a gas pressure below 10 mbar, as shown in figure 4 (curve 2),

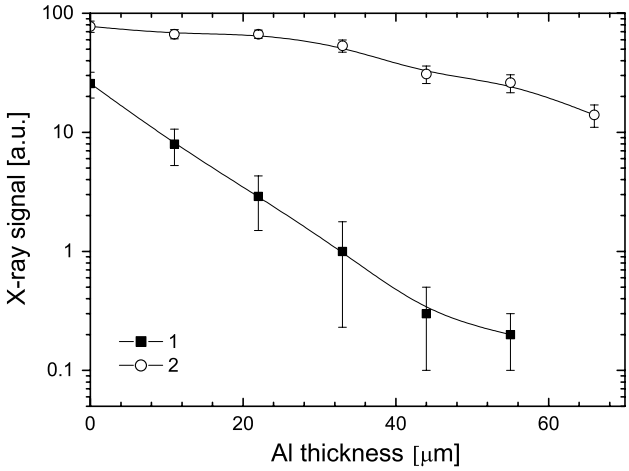

Figure 8. Attenuation curve of the x-ray signal generated in the Al foil target. Discharge in He at $p = 40$ (1) and 20 mbar (2), charging voltage 15 kV.

because we did not perform measurements in this region for this particular set of measurements.

For a preliminary estimation of the mean photon energy of the generated x-rays we measured the attenuation of the x-rays through an increasing number of Al foils. For a monochromatic beam the attenuation increases exponentially with the number of foils. The rate of this exponential increase is determined by the mass absorption coefficient, which depends on the photon energy. For a non-monochromatic spectrum the total attenuation is the sum of the attenuation coefficients of all components of the spectrum.

Two examples of measured attenuation curves are shown in figure 8. The x-rays were produced with a charging voltage of 15 kV, and a He pressure of 40 mbar (lower trace) and with 20 mbar (upper trace). As will be discussed later, we observe only the high-energy part of the bremsstrahlung spectrum (several keV wide) in our experiments. These photons can be produced only by high-energy electrons with an energy close to the maximal energy, and one can expect that the maximum electron energy should decrease monotonically with rising pressure (when the charging voltage is held constant). This can be seen in figure 8. It corresponds to a mean x-ray photon energy of ∼4 keV in 40 mbar He and 6 keV in a He pressure of 20 mbar. Further experiments and a more detailed analysis of the attenuation curves are required for a better estimation of the x-ray spectrum. The preliminary results show, however, that x-ray photons are generated with an energy that is comparable to the charging voltage multiplied with the electron charge.

4. Discussion of the results

It is well known that low energetic x-rays can originate from characteristic or bremsstrahlung radiation. In the following paragraph it will be argued that the x-rays produced in our device do not consist of characteristic radiation. The 0.1 mm Kapton foil output window, the open air gap between the discharge chamber and the photomultiplier housing with the Al foil used as the input filter to the photomultiplier housing provide a certain cut-off photon energy, $E_{\min}$, only above which x-ray photons reach the scintillator and are detectable. For an

estimation of $E_{\min}$, we took the mass absorption coefficients of Al and air provided by Hubbell and Seltzer in the NIST database [7]. For the Kapton foil we used the data from [7] for similar kinds of plastics, as the exact absorption coefficient of the used foil was not known. From this we calculated that all x-ray photons in the 1 keV region are absorbed on the path to the detector, more than 96% of the photons in the 3 keV-range, while for photons with a photon energy of 5 keV only ∼40% is absorbed. This yields a value for the cut-off energy of $E_{\min} \sim 3.5$ keV. This is to be compared with the energy of the characteristic K_α lines of Ar (2.96 keV), Ne (0.849 keV) and Al (1.49 keV) [8], which all have a lower energy than the estimated cut-off energy. Also characteristic radiation of He by decay to the ground state can be excluded because in our experiment the probability of ionization from the inner shell of the excited 1s2s state is rather low, and also because here the photon energy is low compared with the cut-off energy. Thus, although characteristic radiation is produced either in the gas or in the Al target, however, it is too soft to leave the chamber and it is absorbed by the Kapton output window almost entirely.

In contrast, bremsstrahlung shows a continuous spectrum reaching up to the maximum electron energy in the e-beam. What can be detected with our setup is thus the fraction of the high-energy tail of the bremsstrahlung spectrum, extending from $E_{\min}$ to the maximum electron energy, which is a few keV wide. From experimental data [9] and theoretical estimations [10, 11] based on the Kramers cross-section [12] it can be expected that in our experiments, where the narrow high-energy part of the bremsstrahlung x-ray radiation from a thick target is observed, the x-ray signal should increase with the energy of the electrons, E, and the atomic number, Z, of the stopping medium. Additionally, the signal should be proportional to the electron flux and thus to the electron beam current density J.

An important issue is the dependence of the upper limit of the x-ray photon energy on the e-beam parameters. The upper limit of kinetic energy for electrons in the beam is related but not equal to the charging voltage. Rather, the maximum accelerating voltage (potential difference between the cathode and the anode) corresponds to the breakdown voltage of the gas. In figure 3 of [2] it is shown that for any fixed gas pressure the breakdown voltage increases with the charging voltage, but for any fixed charging voltage the breakdown voltage decreases with a pressure increase. This is due to the pulsed mode operation where the non-zero discharge formation time allows a very high voltage over the discharge gap provided it can be applied in a time shorter than the discharge formation time. In fact, most of the fast electrons are produced in the cathode sheath, where the accelerating voltage differs from the breakdown one. However, the breakdown voltage determines the maximum available kinetic energy of the electrons as well as it affects the average energy of them.

The current density of the e-beam depends on the gas pressure and the charging voltage, as has been reported in [2] and figure 4 therein. Specifically, for any fixed gas pressure a higher charging voltage leads to a higher e-beam current density. For any fixed charging voltage the e-beam current density increases up to a certain maximum and then decreases with the pressure. This observation, and the pressure dependence of the electron energy described above, is consistent with the pressure dependence of the x-ray signal measured here (figures 4–7) and qualitatively explains the increase in the observed x-ray signal with increasing charging voltage (see figure 3). It also indicates that our system can be improved considerably by applying a high-voltage pulse with a rise time in the order of nanoseconds.

Another observation mentioned above is that the produced x-ray signal is higher in a stopping medium with a higher Z under otherwise equal conditions. The electron stopping power in Al is much higher than the stopping power of rarified matter (e.g. gases at moderate pressure). In our experiments the penetration depth of fast electrons in the used gases, under the conditions where the maximum x-ray signal is observed, is much higher than the gap between the mesh anode and the Al foil target. Correspondingly, one can neglect the energy loss of the e-beam in front of the Al target such that almost all energy of the e-beam is dissipated in the Al target. The maximum x-ray signal generated with the Al target in the discharge chamber is the same, irrespective of the gas that is used (see figure 6), but this maximum x-ray signal is observed at lower pressure for a heavier gas. From this we can conclude that the same e-beam parameters (current density and electron energy) occur in the discharges with He, Ne and Ar, however, at lower pressure for the heavier gas. This explains why the maximum x-ray signal produced directly in gases, i.e., without Al target (figures 4, 5 and 7), is observed at lower pressure for the heavier gas as well. The observed difference in the maximal x-ray signal amplitude from electron deceleration in the Al target and in He, Ne and Ar (figures 4–7) can be explained by the difference in the atomic number Z of the media. With a Z-number for He of 2 the lowest x-ray signal is produced directly in He without Al target. The Z-number of Al is 13 and the x-ray signal observed is higher under the same conditions (figure 4). Ne and Al have close Z-number values (10 and 13 correspondingly) and the observed signal is almost the same (see figure 5). It is expected that for Al the signal should be stronger because of a higher Z, but we see only a slightly smaller signal. This can be explained by the geometry of the generation scheme. When electrons are stopped by the Al foil, the x-ray radiation comes from one thin plane. When the electrons are stopped by Ne (no foil), the radiation source is distributed along the path of the electrons in the gas. The windows (4 and 8 in figure 1) form a narrow solid angle for the observation and determine the amount of radiation detected. So for a distributed source of radiation (without the Al foil) the 'effective' solid angle is larger. Thus the largest signal is observed when x-rays are generated directly in Ar ($Z = 18$) without Al target.

If one normalizes the data of figure 7 to the Z numbers of He ($Z = 2$), Ne ($Z = 10$) and Ar ($Z = 18$) and makes a graph with $p \times Z$ (the electron energy loss: Bethe's formula [13] $\mathrm{d}E/\mathrm{d}x \sim n \times Z \sim p \times Z$) and the x-ray signal/$Z$ as coordinates, we expect that all the three curves should coincide. The result of this normalization is shown in figure 9. The curves for Ne (2) and Ar (3) coincide quite well, taking into account the error bars and quantitative nature of these assumptions. However, for He (1) the resulting curve for the maximum signal/Z value is a bit higher than expected.

From our measurements we can conclude that a higher charging voltage will produce a more intense x-ray beam and also the upper energy limit of the generated x-ray photons

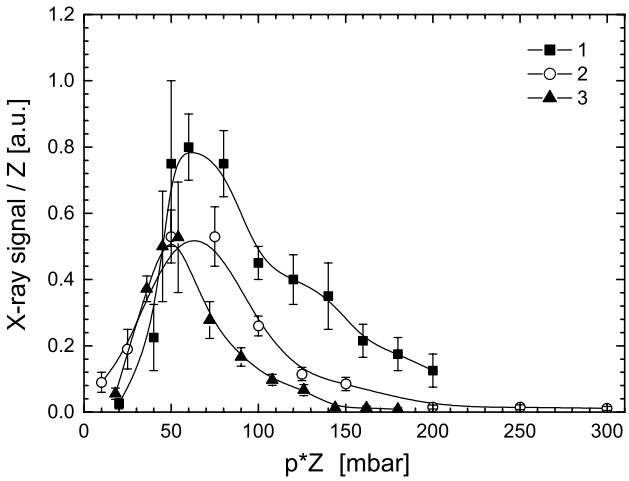

Figure 9. Dependence of the normalized x-ray signal amplitude generated in gases without an Al foil target on the normalized gas pressure. Charging voltage is 15 kV. 1: He, 2: Ne, 3: Ar.

increase with the applied voltage. We have argued before that by using a voltage pulse with a much shorter rise time it should be possible to apply a significantly higher voltage over the same discharge gap. In our experiments the rise time of the voltage pulse was ∼80 ns, so by decreasing the voltage rise time in our device to the ns level we expect to generate electrons with a kinetic energy in the order of 50–100 keV. For preionization of the active volume of multi-atmospheric gas (excimer) lasers x-ray radiation must penetrate the laser chamber through a foil capable of withstanding a pressure difference of several bars. It implies that the energy of the x-ray photons should be in the order of 50–100 keV. It is expected that by the proposed modification not only the electron (and thus x-ray photon) energy but also the current density will increase significantly at higher operating voltages.

5. Conclusion

In this work we report about a stable, reliable, reproducible and simple soft x-ray source. It has been shown that a fast electron beam produced in an open barrier discharge generates x-ray radiation due to the bremsstrahlung process. The device is able to operate at a high repetition rate of up to several kHz. The production of bremsstrahlung occurs when fast electrons are stopped by a metal target or directly in a gas. The x-ray intensity strongly depends on the parameters of the electron beam (electron energy and current density) and the stopping material properties (Z-number). It appears that the energy of the x-ray photons is comparable to the applied discharge voltage. The highest obtained energy in the x-ray spectrum depends on the electron energy (∼10 keV in the investigated case) and the lowest energy is determined by the transmittance of the output window and the window of the detector.

In [1, 2] it was concluded that fast electrons are generated in a high-voltage barrier discharge. This conclusion was made from the observation of the glow of the gas, excited by the beam of electrons, and from the estimation of the electron penetration depth in the gas, based on the gas glow. In [2] the electron beam current density and in [3] the extremely high energy efficiency of the e-beam generation (∼90%) in this type of open barrier discharge were measured, but no information on the electron energy in the beam was given. In this paper the generation of soft x-rays during the deceleration of the e-beam finally proves the presence of fast electrons (∼10 keV) produced in this high-voltage barrier discharge. By applying a 50–100 kV voltage pulse with a much shorter rise time we expect a considerable enhancement of electron beam intensity with a kinetic energy for the electrons of 50–100 keV. Such a source is extremely well suited as a preionization source for high-pressure gas lasers.

Acknowledgments

The authors appreciate the stimulating interest of Dr S V Mitko during the course of these experiments. This research is supported by the Technology Foundation STW, applied science division of NWO and the technology programme of the Ministry of Economic Affairs.

References

[1] Azarov A V, Mitko S V and Ochkin V N 2002 *Quantum Electron.* **32** 675
[2] Mitko S V, Udalov Y B, Peters P J M, Ochkin V N and Boller K-J 2003 *Appl. Phys. Lett.* **83** 2760
[3] Mitko S V, Oudalov A Yu, Udalov Yu B, Peters P J M and Boller K-J 2005 *Rev. Sci. Instrum.* **76** 013101
[4] Bokhan P A and Zarkevsky D E 2002 *Tech. Phys. Lett.* **28** 454
[5] Sorokin A R 2003 *Tech. Phys. Lett.* **10** 836
[6] Babych L P 2003 *High-Energy Phenomena in Electric Discharges in Dense Gases: Theory, Experiment and Natural Phenomena* (*ISTC Science and Technology Series* vol 2) (Arlington, VA: Futurepast)
[7] Hubbell J H 1982 *Int. J. Appl. Radiat. Isot.* **33** 1269
Seltzer S M 1993 *Radiat. Res.* **136** 147
[8] Bearden J A 1967 *Rev. Mod. Phys.* **39** 78–124
Schweppe J, Deslattes R D, Mooney T and Powell C J 1994 *J. Electron Spectrosc. Relat. Phenom.* **67** 463–78
[9] Mohr P J and Taylor B N 2000 *Rev. Mod. Phys.* **72** 351
[10] Chervenak J G and Liuzzi A 1975 *Phys. Rev.* A **12** 26
[11] Lamoureux M, Waller P, Charles P and Avdonina N B 2000 *Phys. Rev.* E **62** 4091
[12] Kramers H A 1923 *Phil. Mag.* **46** 836
[13] Bethe H 1930 *Ann. Phys.*, Lpz. **5** 325